A graph deep learning model for the classification of groups with different IQ using resting state fMRI

Qu, Gang, Hu, Wenxing, Xiao, Li, Wang, Yu-Ping

Gang Qu, Wenxing Hu, Li Xiao, Yu-Ping Wang, "A graph deep learning model for the classification of groups with different IQ using resting state fMRI," Proc. SPIE 11317, Medical Imaging 2020: Biomedical Applications in Molecular, Structural, and Functional Imaging, 113170A (28 February 2020); doi: 10.1117/12.2549274

SPIE.

Event: SPIE Medical Imaging, 2020, Houston, Texas, United States

A graph deep learning model for the classification of groups with different IQ using resting state fMRI

Gang Qu[a], Wenxing Hu[a], Li Xiao[a], and Yu-Ping Wang[a]

[a]Department of Biomedical Engineering, Tulane University, New Orleans, LA, USA

ABSTRACT

Functional connectivity (FC) analysis, which measures the connection between different brain regions, has been widely used to study brain function and development. However, FC-based analysis breaks the local structure in MRI images, resulting in a challenge for applying advanced deep learning models, e.g., convolutional neural networks (CNN). To fit the data in a non-Euclidean domain, graph convolutional neural network (GCN) was proposed, which can work on graphs rather than raw images, making it a suitable model for brain FC study. The small sample size is another challenge. Compared with natural images, medical images are usually limited in data sample size. Moreover, labeling medical images requires laborious annotation and is time-consuming. These limitations result in low accuracy and overfitting problem when training a conventional deep learning model on medical images. To address this problem, we employed a semi-supervised GCN with a Laplacian regularization term. By exploiting the between-sample information, semi-supervised GCN can achieve better performance on data with limited sample size. We applied the semi-supervised GCN model to a brain imaging cohort to classify the groups with different Wide Range Achievement Test (WRAT) scores. Experimental results showed semi-supervised GCN can improve classification accuracy, demonstrating the superior power of semi-supervised GCN on small datasets.

Keywords: GCN, Functional magnetic resonance imaging, brain functional networks, WRAT

1. INTRODUCTION

Neuroimaging has been widely used to study human brain function and development.[1] Compared with structural imaging which can be used for diagnosis of intracranial disorder and damage,[2] there is more interest in functional imaging which can be used for diagnosis of much finer disorder (e.g., metabolic diseases and lesions[3]). Functional magnetic resonance imaging (fMRI) measures blood-oxygen-level-dependent (BOLD) contrast signals which are highly related to brain cells' energy activity. To study the connectivity and neurophysiological events across different brain regions, the correlation across different regions of interest can be defined as functional connectivity.[4] Functional connectivity[5] has been successfully used to analyze the statistical patterns of brain activity and shown great potential for the study of cognitive psychology and physical development of the human brain.[6]

Different brain regions function and harmonize in a connected network. Region-region based network study has been shown powerful to analyze brain functions. However, region-region network breaks image structure and is not appropriate to implement image based methods. To deal with data in non-Euclidean domain and to capture the complex relationships between features, graph convolutional neural network (GCN) was proposed by many researchers.[7] By incorporating complex geometric structures of graphs, GCN can broadcast the labels based on the relationships between different nodes. In other words, by investigating the links between subjects, GCN has the ability of reasoning the labels from nearby nodes. This enables GCN to handle data with a small sample size, which is ideal for our Philadelphia Neurodevelopmental Cohort (PNC) datasets.

Further author information: (Send correspondence to Yu-ping Wang)
E-mail: wyp@tulane.edu.

Medical Imaging 2020: Biomedical Applications in Molecular, Structural, and Functional Imaging, edited by Andrzej Krol, Barjor S. Gimi, Proc. of SPIE Vol. 11317, 113170A · © 2020 SPIE · CCC code: 1605-7422/20/$21 · doi: 10.1117/12.2549274

2. METHODOLOGY

2.1 Graph Convolution

Graph, which is a generalized data structure, can be used for non-euclidean data representation. A graph can be denoted as $\mathcal{G} = (\mathcal{V}, \mathcal{E})$ with the node set $\mathcal{V} = \{\mathbf{v}_1, \mathbf{v}_2 \cdots \mathbf{v}_N\}$ and the edge set $\mathcal{E}$. Edges represent the connectivity and relations between the nodes. Here, we assume that the graph $\mathcal{G}$ is weighted and undirected. The graph Laplacian for an undirected graph can be written in the normalized form as

$$\mathbf{L}_{norm} := \mathbf{I}_N - \mathbf{D}^{-\frac{1}{2}}\mathbf{A}\mathbf{D}^{-\frac{1}{2}}, \tag{1}$$

where $\mathbf{A} \in \mathbb{R}^{N\times N}$ is the adjacency matrix, and $\mathbf{D}$ is the degree matrix which is a diagonal matrix with each diagonal element being the sum of the values in its respective row of $\mathbf{A}$, i.e., $\mathbf{D}(i,i) = \sum_j \mathbf{A}(i,j)$. $\mathbf{L}_{norm}$ is a real symmetric positive-semi-definite matrix.[8] Using eigen-decomposition, we can rewrite the graph Laplacian into $\mathbf{L}_{norm} = \mathbf{U}\mathbf{\Lambda}\mathbf{U}^T$, where $\mathbf{\Lambda}$ is a diagonal matrix with diagonal elements $\mathbf{\Lambda}(i,i)$ being the eigenvalues of $\mathbf{L}_{norm}$, and $\mathbf{U}$ is the orthogonal matrix of eigenvectors. Similar to the Fourier theory, the graph Fourier transform (GFT), the inverse GFT, and the graph convolution are defined based on the spectrum of the graph Laplacian (see[9] for details). Specifically, the graph convolution between the signal f and filter g_θ can be defined as follows,

$$f * g_\theta = \mathbf{U}((\mathbf{U}^T g_\theta) \odot (\mathbf{U}^T f)) = (\mathbf{U} g_\theta \mathbf{U}^T) f, \tag{2}$$

where g_θ refers to a graph spectral filter parameterized by $\theta \in \mathbb{R}^N$, as we will illustrate in detail below.

2.2 Pipeline to build the GCN

To implement GCN, our datasets need to be converted to graph structure. Alternatively, we can construct an affinity graph using similarity function to compute the weights for edges. Let $\mathbf{X} \in \mathbb{R}^{N\times Dim}$ be the input of our model, where N is the number of subjects, and each row of X denotes the vectorization of the functional connectivity matrix of the corresponding subject. We then construct a subject-subject graph and calculate the adjacency matrix $\mathbf{A}$ as

$$\mathbf{A}(i,j) = exp(-\frac{\|\mathbf{X}(i,) - \mathbf{X}(j,)\|^2}{2\rho^2}), \tag{3}$$

where ρ is the standard deviation calculated by $\mathbf{X}$(i,) and $\mathbf{X}$(j,), which refer to the i_{th} and the j_{th} row of $\mathbf{X}$, respectively.

The key idea of graph convolution neural network is based on the spectral decomposition of Laplacian matrix $\mathbf{L}_{norm}$ as in Eq.1. According to the definition of graph convolution, we can define the graph convolution layer[10] as follows,

$$\mathbf{H}^{(l+1)} = \sigma((\mathbf{U} g_\theta \mathbf{U}^T)\mathbf{H}^{(l)}), \tag{4}$$

where $\mathbf{H}^l$ is the l_{th} hidden layer and $\mathbf{H}^0 = \mathbf{X}$, and σ is the activation function[10,11].

In order to incorporate the graph structure, we need to design a filter g_θ as a function of the eigenvalues of graph Laplacian. To reduce the computational cost, g_θ can be approximated as a truncated expansion in terms of polynomials, e.g., Chebyshev polynomials[11] The K_{th} order polynomial is related to n length walks of the graph.[12] We set the local "receptive field" as K walks from the central nodes to neighbors, which is similar to the kernel size in Convolutional Neural network. According to the work,[11] we can use Chebyshev polynomial to further improve the computational efficiency as

$$g_\theta(\mathbf{\Lambda}) = \sum_{k=0}^{K-1} \boldsymbol{\theta}'_k T_k(\tilde{\mathbf{\Lambda}}), \tag{5}$$

where $T_k(x)$ is the K_{th} order polynomial with $T_0 = 1$ and T_1=x, $\tilde{\mathbf{\Lambda}}=\frac{2}{\max_{1\le i\le N}(\mathbf{\Lambda}(i,i))}\mathbf{\Lambda} - \mathbf{I}_N$, $\theta'_k \in \mathbb{R}^N$ is Chebyshev coefficients. Accordingly, we can further approximate the g_θ as

$$g_\theta = \boldsymbol{\theta}(\tilde{\mathbf{D}}^{-\frac{1}{2}}\tilde{\mathbf{A}}\tilde{\mathbf{D}}^{-\frac{1}{2}}), \tag{6}$$

with $\tilde{\mathbf{A}} = \mathbf{A} + \lambda\mathbf{I}_N$, where λ is the constant coefficient (λ is set to be 1), and $\tilde{\mathbf{D}}$ is a diagonal matrix with each diagonal element being the sum of the values in its respective row of $\tilde{\mathbf{A}}$, $\tilde{\mathbf{D}}(i,i) = \sum_j \tilde{\mathbf{A}}(i,j)$, $\boldsymbol{\theta}=\boldsymbol{\theta}'_{\mathbf{0}} - \boldsymbol{\theta}'_{\mathbf{1}}$. The Eq.4 can be rewritten as follow:

$$\mathbf{H}^{(l+1)} = \sigma(\tilde{\mathbf{D}}^{-\frac{1}{2}}\tilde{\mathbf{A}}\tilde{\mathbf{D}}^{-\frac{1}{2}}\mathbf{H}^{(l)}\mathbf{W}^l), \tag{7}$$

where $\mathbf{W}$ represents the weight matrix for the l_{th} hidden layer.

3. EXPERIMENT

3.1 PNC Data

The Philadelphia Neurodevelopmental Cohort (PNC) datasets were used for our experiment. The dataset has resting-state fMRI (rs-fMRI) data, collected from 857 subjects. The duration of the rs-fMRI scan was 6.2 minutes (124 TR), during which subjects were asked to stay still and keep awake. SPM12 * was used to conduct motion correction, spatial normalization and smoothing with a 3mm Gaussian kernel. Multiple regressions were used and the influence of motion was considered.[13] As the result, we got 264 regions of interest (ROIs) based on the Power coordinates template.[14] Subjects were categorized into high and low WRAT groups following the setting in work.[15] More specifically, the top and bottom 20% comprised High and Low cognitive groups, respectively. Principal components analysis (PCA) was used on $\mathbf{X}$ before inputting our model for dimension reduction, with confidence score > 0.9.

3.2 Experimental setup

we show the whole pipeline of our approach in Fig.1. During the training, we calculated the loss function as Eq.8 only for

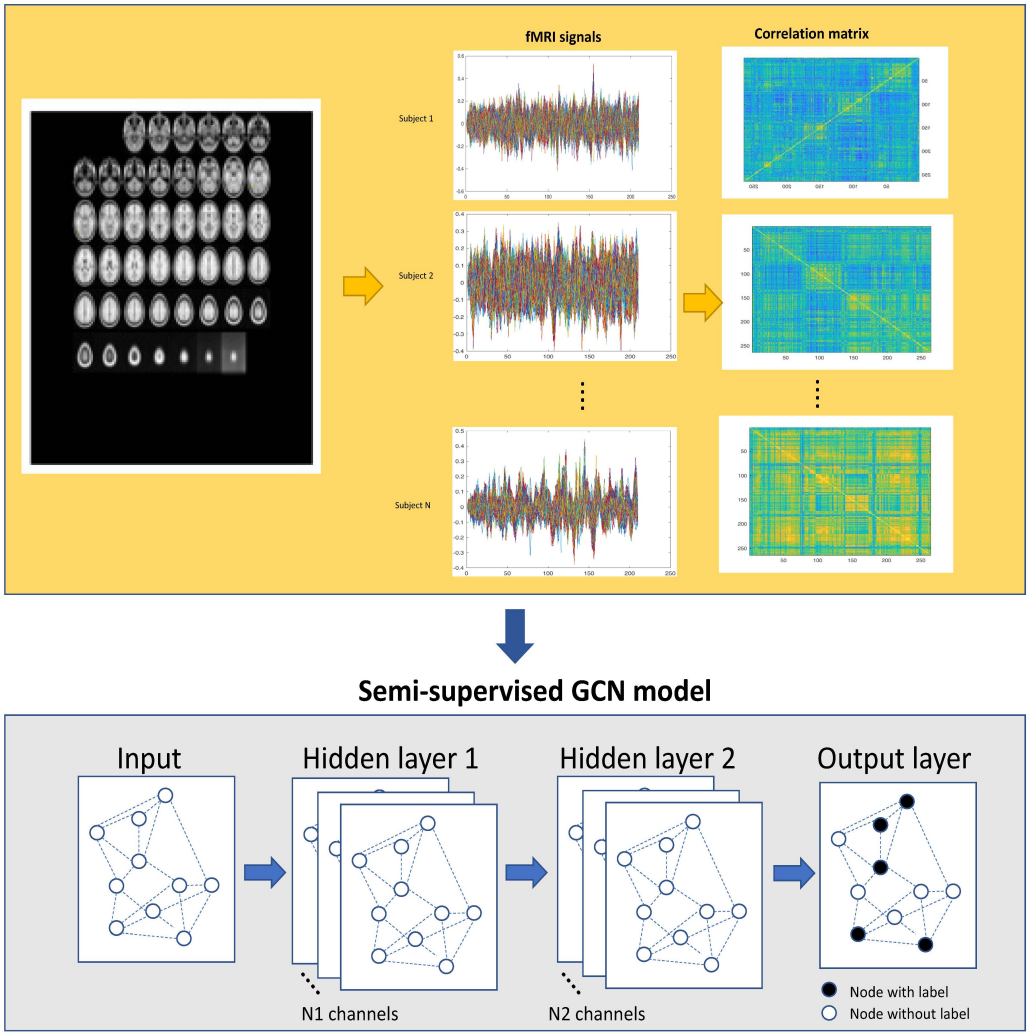

Figure 1: The flowchart of the proposed framework in this study. The upper part is data processing step and the lower part is the semi-supervised GCN model

*http://www.fil.ion.ucl.ac.uk/spm/software/spm12/

the nodes with labels, and the nodes without labels shared the same weights during the validation.

$$Loss = -\sum_{d\in Y_D}\sum_{f=1}^{F} Y_{df} lnZ_{df} + \lambda_1 R_{L_{reg}} + \lambda_2 R_{L_2},$$
$$R_{L_{reg}} = \frac{1}{2}\sum_{i,j}^{N} \mathbf{A}(i,j)\left(\frac{\hat{y_i}}{\sqrt{\mathbf{D}(i,i)}} - \frac{\hat{y_j}}{\sqrt{\mathbf{D}(j,j)}}\right)^2, \quad (8)$$

where Y_{df} denotes the set of nodes with labels, F refers to the number of classes and is set to 2 as the experiment is a binary classification task, Z_{df} represents the predicted value ranged in [0,1]. R_{L_2} and $R_{L_{reg}}$ refer to the l_2 and Laplacian regularization, respectively. We trained a GCN with 3 hidden layers and 1024, 512, 512 channels in each layer, respectively. We set $\lambda_1 = 5e-3$, $\lambda_2 = 1e-4$, and the learning rate to be $1e-5$. The models were trained on a desktop with an Intel(R) i7-8700KProcessor, and a NVIDIA GeForce GTX 1080 GPU.

3.2.1 WRAT Classification

We applied GCN to resting paradigms fMRI and compared the performance with other models including support vector machine (SVM) and multi-layer perceptron (MLP). We randomly labeled 50 % nodes on the graph. For SVM and MLP, we randomly separate 50% subjects as training and the rest as testing for a fair comparison. Each experiment was repeated 10 times by re-sampling, and we calculated the means and standard deviations. As shown in Table 1, SVM achieved similar predictive performance as MLP, while GCN outperformed both SVM and MLP.

3.3 Visualization

To visualize the model, we used t-distributed stochastic neighbor embedding (t-SNE) to map the high dimensions data to low dimensions (2D). Since we only used one neuron at the fourth layer (output layer), t-SNE was applied to the first layer, the second layer, and the third layer of GCN. The result was shown in Figure.2.

From the first layer to the third layer, we can see the nodes began to be clustered into two classes. The distance between the two classes became larger. However, there were still some subjects mixed.

Table 1: The classification accuracy result with different models. CORR: Vectorized correlation matrix, DM: Diffusion map, SRC: Spase coding, DT: Decision tree

Paradigm	CORR+SVM	PCA+SVM	DM+SVM	PCA+SRC	PCA+DT	PCA+MLP	**PCA+GCN**
Rs-fMRI	0.65±0.02	0.56±0.01	0.55±0.01	0.56±0.01	0.57±0.01	0.66±0.01	**0.68±0.01**

4. DISCUSSION

As a generalized convolutional network model, GCN enables us to capture complicated data structure in non-Euclidean data domain. Graph relaxes the requirement for strong local structure in Euclidean domain, which is essential for CNN. Because of that, graph-based deep learning models can achieve better interpretability than conventional networks such as CNN and RNN. This makes GCN more suitable for brain network analysis. To our knowledge, our work represented the first attempt to apply the GCN to brain functional connectivity study. By constructing a subject-subject graph, we investigated both brain connectivity and its prediction on human cognitive ability. According to results, the GCN achieved the highest classification accuracy compared to MLP and SVM. Higher accuracy of classifying cognitive groups demonstrated that GCN, along with fMRI based brain fingerprints, can be used to study the brain function and human cognitive ability.

Acknowledgment

The authors would like to thank the NIH (R01 GM109068, R01 MH104680, R01 MH107354, P20 GM103472, R01 REB020407, R01 EB006841) and NSF (#1539067) for the partial support.

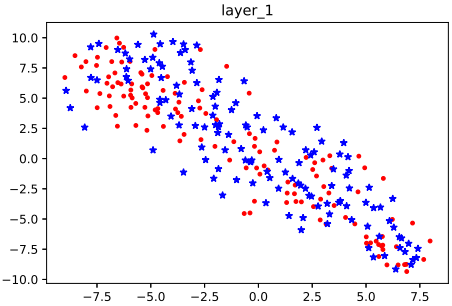

(a) The first layer of GCN

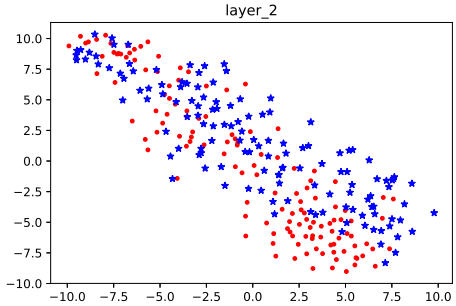

(b) The second layer of GCN

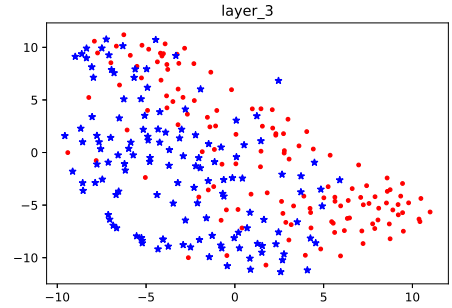

(c) The Third layer of GCN

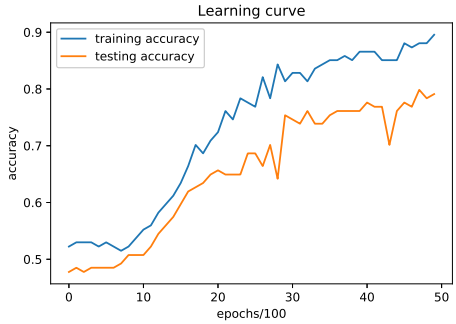

(d) The learning curve

Figure 2: (a), (b), (c) show the visualization of GCN: red dots represent subjects with high WRAT scores; blue asterisks represent subjects with low WRAT scores. From the first layer to the third layer, two groups are clustered more discriminatively. (d) shows training accuracy and testing accuracy

REFERENCES

[1] Casey, B., Giedd, J. N., and Thomas, K. M., "Structural and functional brain development and its relation to cognitive development," *Biological psychology* **54**(1-3), 241–257 (2000).

[2] Crosson, B., Ford, A., McGregor, K. M., Meinzer, M., Cheshkov, S., Li, X., Walker-Batson, D., and Briggs, R. W., "Functional imaging and related techniques: an introduction for rehabilitation researchers," *Journal of rehabilitation research and development* **47**(2), vii (2010).

[3] Carolyn Cidis Meltzer, M., Smith, G., DeKosky, S. T., Pollock, B. G., Mathis, C. A., Moore, R. Y., Kupfer, D. J., Reynolds, C. F., et al., "Serotonin in aging, late-life depression, and alzheimers disease: the emerging role of functional imaging," *Neuropsychopharmacology* **18**(6), 407–430 (1998).

[4] Biswal, B. B., Kylen, J. V., and Hyde, J. S., "Simultaneous assessment of flow and bold signals in resting-state functional connectivity maps," *NMR in Biomedicine* **10**(4-5), 165–170 (1997).

[5] Calhoun, V. D. and Adali, T., "Time-varying brain connectivity in fmri data: whole-brain data-driven approaches for capturing and characterizing dynamic states," *IEEE Signal Processing Magazine* **33**(3), 52–66 (2016).

[6] Pascual-Leone, A., Walsh, V., and Rothwell, J., "Transcranial magnetic stimulation in cognitive neuroscience–virtual lesion, chronometry, and functional connectivity," *Current opinion in neurobiology* **10**(2), 232–237 (2000).

[7] Bruna, J., Zaremba, W., Szlam, A., and LeCun, Y., "Spectral networks and locally connected networks on graphs," *arXiv preprint arXiv:1312.6203* (2013).

[8] Belkin, M. and Niyogi, P., "Laplacian eigenmaps and spectral techniques for embedding and clustering," in [*Advances in neural information processing systems*], 585–591 (2002).

[9] Sandryhaila, A. and Moura, J. M., "Discrete signal processing on graphs: Graph fourier transform," in [*2013 IEEE International Conference on Acoustics, Speech and Signal Processing*], 6167–6170, IEEE (2013).

[10] Kipf, T. N. and Welling, M., "Semi-supervised classification with graph convolutional networks," *international conference on learning representations* (2017).

[11] Defferrard, M., Bresson, X., and Vandergheynst, P., "Convolutional neural networks on graphs with fast localized spectral filtering," in [*Advances in neural information processing systems*], 3844–3852 (2016).

[12] Harary, F. and Schwenk, A., "The spectral approach to determining the number of walks in a graph," *Pacific Journal of Mathematics* **80**(2), 443–449 (1979).

[13] Friston, K. J., Frith, C. D., Frackowiak, R. S., and Turner, R., "Characterizing dynamic brain responses with fmri: a multivariate approach," *Neuroimage* **2**(2), 166–172 (1995).

[14] Power, J. D., Cohen, A. L., Nelson, S. M., Wig, G. S., Barnes, K. A., Church, J. A., Vogel, A. C., Laumann, T. O., Miezin, F. M., Schlaggar, B. L., et al., "Functional network organization of the human brain," *Neuron* **72**(4), 665–678 (2011).

[15] Hu, W., Cai, B., Zhang, A., Calhoun, V. D., and Wang, Y.-P., "Deep collaborative learning with application to multimodal brain development study," *IEEE Transactions on Biomedical Engineering* (2019).